Supplementary Materials

Supplementary Figure 1. Cy3 fluorescence image of ZMW immobilization of 70S ribosome initiation complexes with fMet-(Cy3)tRNA^{fMet} and 5'-biotinylated mRNA. The population of fluorescence occupancy increased as the concentration of ribosome complex increased. Blocking neutravidin binding sites by pre-incubation with biotin prevents immobilization in the presence of 100 nM ribosomal complex. The lower right panel shows the fractional Cy3 fluorescence occupancy over all ZMWs at each ribosome complex concentration (red circles), and the fraction of all Cy3 traces with multiple photobleaching steps (blue triangles). Fitting the blue triangles to the Poisson curve $1-\exp(-\lambda x) = 1-\lambda^{k}\exp(-\lambda x)/k!$, where k=0 (blue line) yields a lambda value of 0.006 (red line), 0.0005 (blue line).

Supplementary Figure 2. Surface interaction of translational components with ZMWs (avg. ± s. d.) was tested using ellipsometry on a non-treated aluminum surface (upper left) and on the phosphonate treated surface (upper right). Thickness changes for each surface in nm are shown. The concentration of each component is 1 μM EF-G, 1 μM EF-Tu and 100 μM tRNA^{Phe}. In the absence of phosphonate treatment, tRNA interacts with the aluminum (Al) surface, but this interaction is not observed upon phosphonate passivation. Protein factors and TC do not interact with either surface. The lower panel shows fluorescence traces for ZMWs in the absence of ribosomes for 500 nM fMet-(Cy3)tRNA^{fMet}, 500 nM Phe-(Cy5)tRNA^{Phe}, and 500 nM Phe-(Cy5)tRNA^{Phe} complexed with EF-Tu and GTP. Fluorescent sticking events are exceptionally rare. These results confirm minimal nonspecific surface adsorption of our labeled and unlabeled translation components.

Supplementary Figure 3. tRNA-tRNA FRET (Fluorescence Resonance Energy Transfer) measurement in ZMWs to confirm ribosome function. Single-molecule FRET was measured between fMet-(Cy3)tRNA^{fMet} in the P site and incoming Phe-(Cy5)tRNA^{Phe} in the A site in the absence of EF-G using 532 nm excitation. Phe-(Cy5)tRNA^{Phe} TC was delivered to ribosomal complexes using the MFKF mRNA as reported previously[28,29]. The fluorescence trace shown in the lower left is an example of a FRET measurement. After delivery of TC, detected Cy5 signals were anti-correlated with Cy3 signals, and FRET efficiency is shown in the panel below the fluorescence traces. FRET experiments were repeated under various conditions, with post-synchronized FRET efficiencies as follows: 0.55 for EF-Tu (GTP), 0.35 for EF-Tu (GDPNP), 0.25 for near-cognate MFLF mRNA containing the change from a UUU Phe codon to a CUU Leu codon, and 0.25 for EF-Tu (GTP) in the presence of tetracycline (from top to bottom in the lower right, respectively). FRET efficiencies were suppressed by 0.1-0.2 as compared with previous FRET studies on the ribosome[28,29], due to quenching of Cy5 emission by the ZMW. We confirmed this suppression by comparing FRET efficiencies between Cy3 and Cy5 separated by 17 base pairs in a DNA duplex in ZMWs and in flat-glass TIRF (not shown).

Supplementary Figure 4. tRNA arrival time analysis at different TC concentrations. At 30 nM TC delivery, the average arrival times measured by flat-glass TIRF and ZMW methods are similar. tRNA-tRNA FRET experiments in ZMWs were repeated at TC concentrations ranging from 150 nM-600 nM. As expected, FRET arrival times in ZMWs decreased with increasing TC concentration. Measurements at these concentrations of labeled ligands would not be possible using TIRF due to high background fluorescence.

Supplementary Figure 5. Statistical analysis of pulses (avg. ± s. d.) with the mRNA templates ($M(FK)_6$, $M(FKK)_4$ and MF_{12} at 200 nM TCs and 500 nM EF-G. tRNA transit time (upper left) and time between tRNA arrivals (upper right) showed no significant differences between the various mRNA templates. As expected, erythromycin did not affect the tRNA transit time. We also performed translation using an immobilized 30S initiation complex on $M(FK)_6$ instead of a 70S complex. Delivery of TC was performed as above, but also in the presence of 50S subunits (lower left, compare in Fig 1a). Due to a waiting period for the 50S joining event, the plot of tRNA arrival times (avg. ± s. d.) using the 30S initiation complex had the same slope but was shifted up compared to the plot for the 70S initiation complex.

Supplementary Figure 6. Analysis of tRNA occupancy on translating ribosomes with different mRNA templates. Similar trends of tRNA occupancy are observed for different mRNA templates, and also at lower excitation laser power. tRNA occupancy analysis with various mRNA templates and with two different laser powers at 200 nM TC and 500 nM EF-G (compare to Fig. 5b).

Supplementary Figure 7. Translation experiment at 1000 nM Phe-(Cy5)$tRNA^{Phe}$ and 200 nM Lys-(Cy2)$tRNA^{Lys}$ delivery. Cy5 overlapping is observed after delivery. Two-dimentional histograms are post-synchronized in time with respect to each tRNA transit event. At the 5^{th} F codon, 3 tRNA occupancy was observed.

References

28. S. C. Blanchard, R. L. Gonzalez, H. D. Kim, S. Chu, J. D. Puglisi, *Nat Struct Mol Biol* **11**, 1008 (Oct, 2004).

29. S. C. Blanchard, H. D. Kim, R. L. Gonzalez, Jr., J. D. Puglisi, S. Chu, *Proc Natl Acad Sci U S A* **101**, 12893 (Aug 31, 2004).

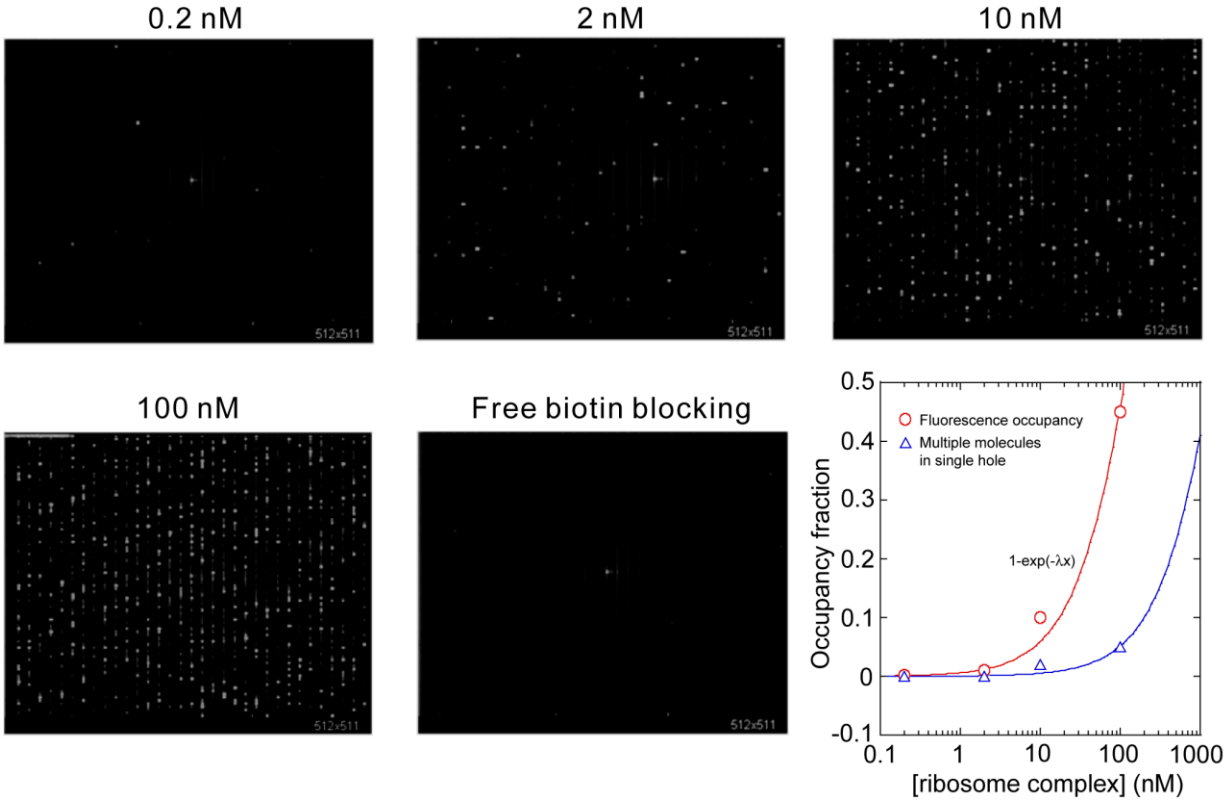

Supplementary figure. 1

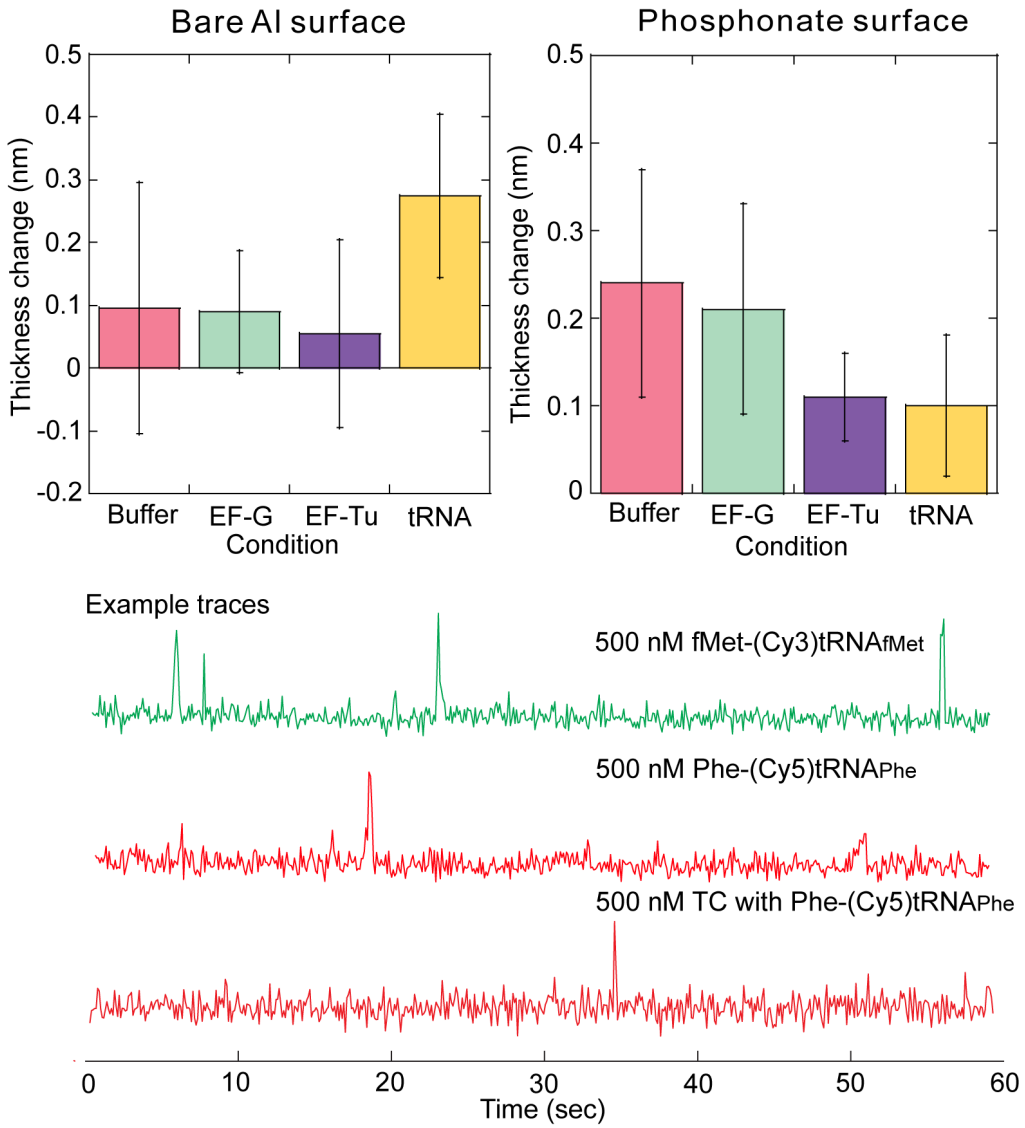

Supplementary figure. 2

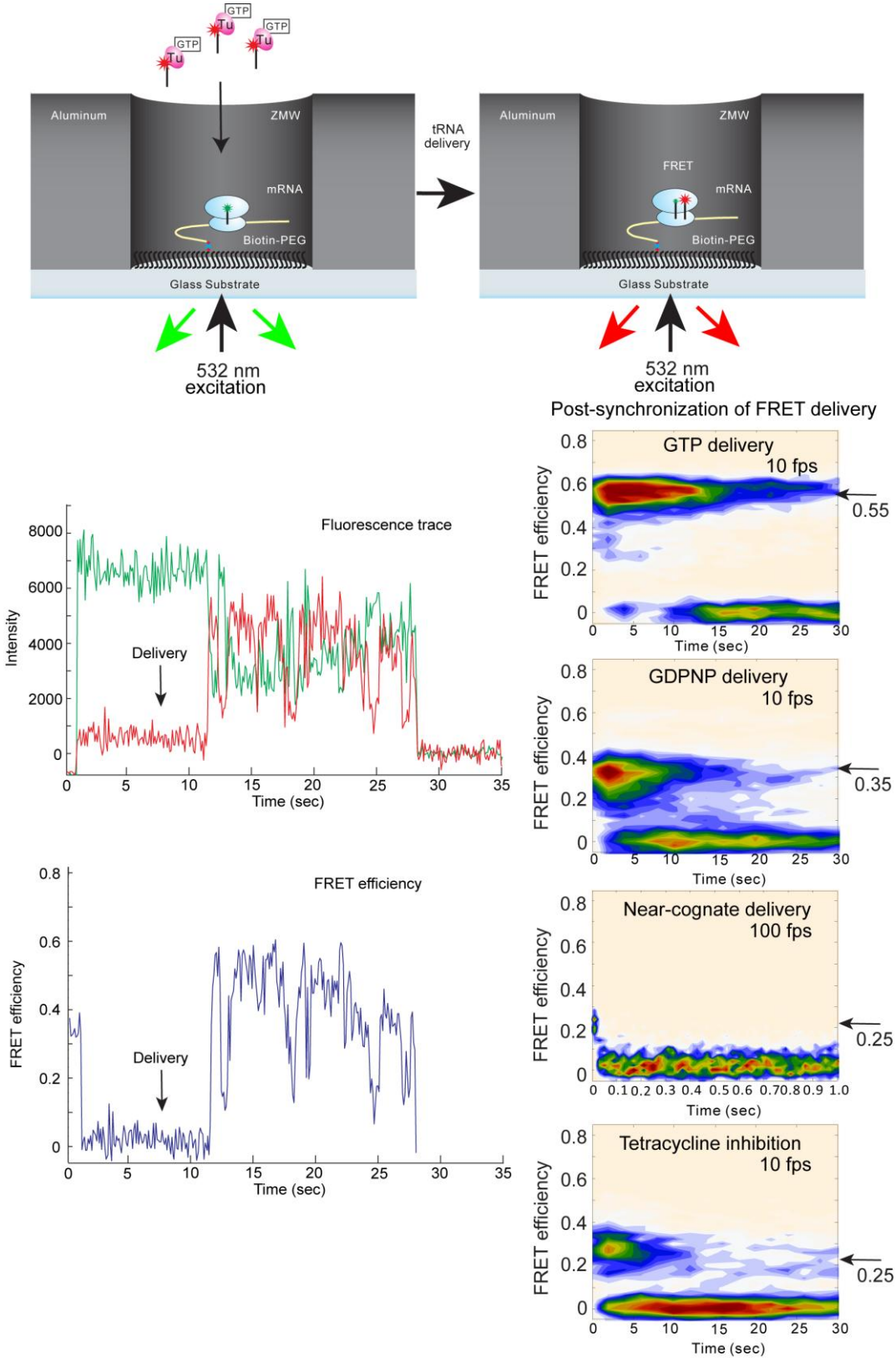

Supplementary figure. 3

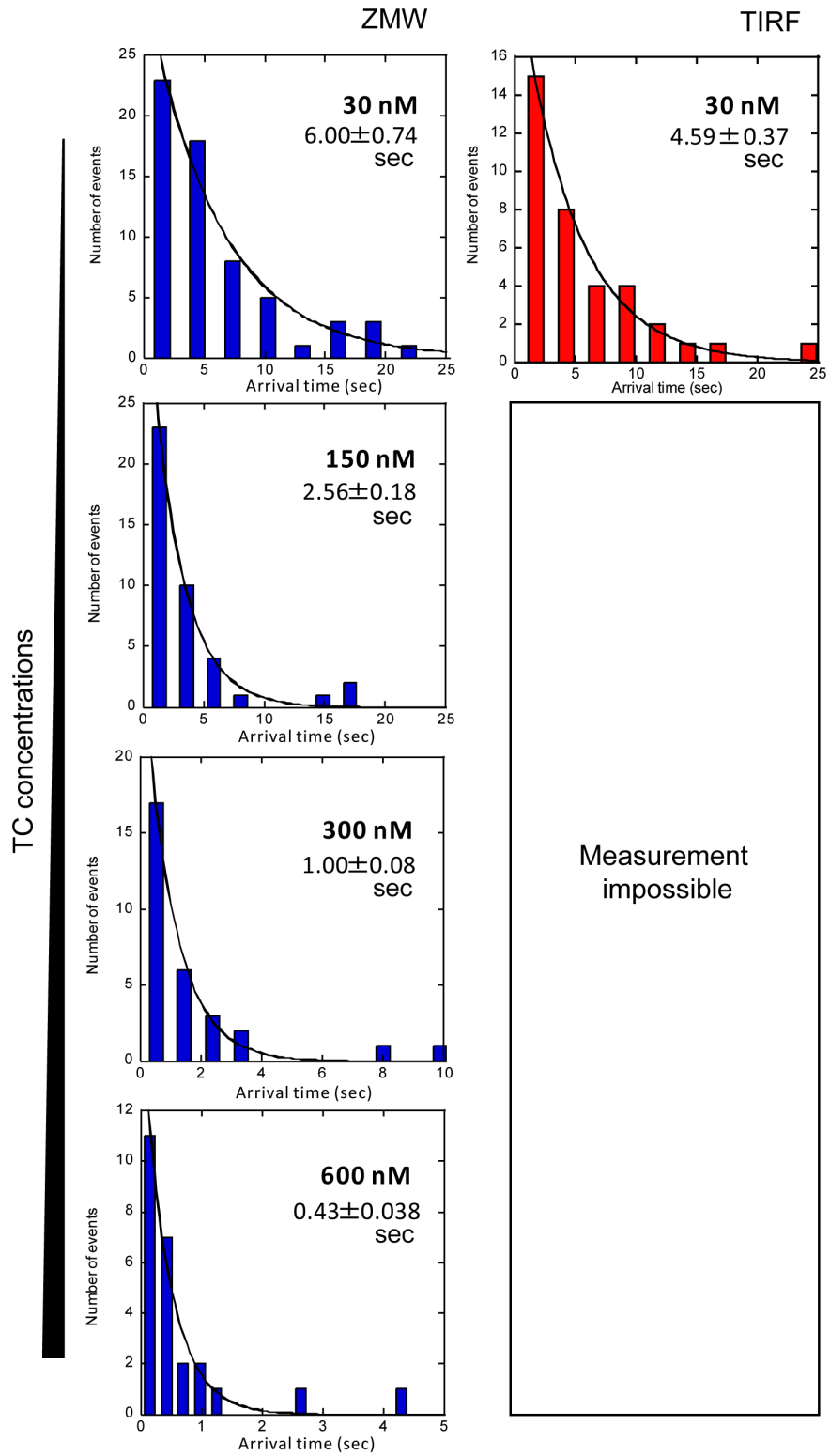

Supplementary figure. 4

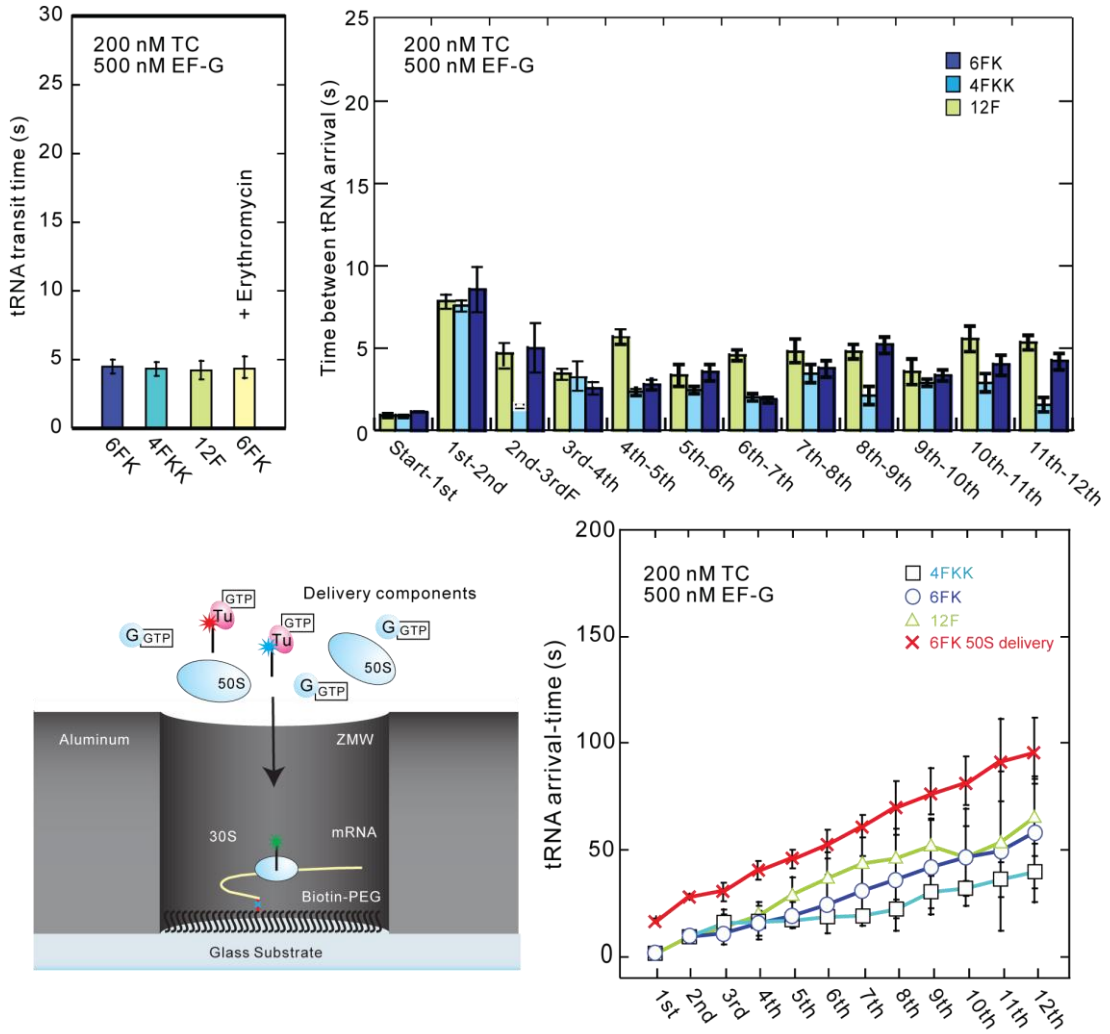

Supplementary figure. 5

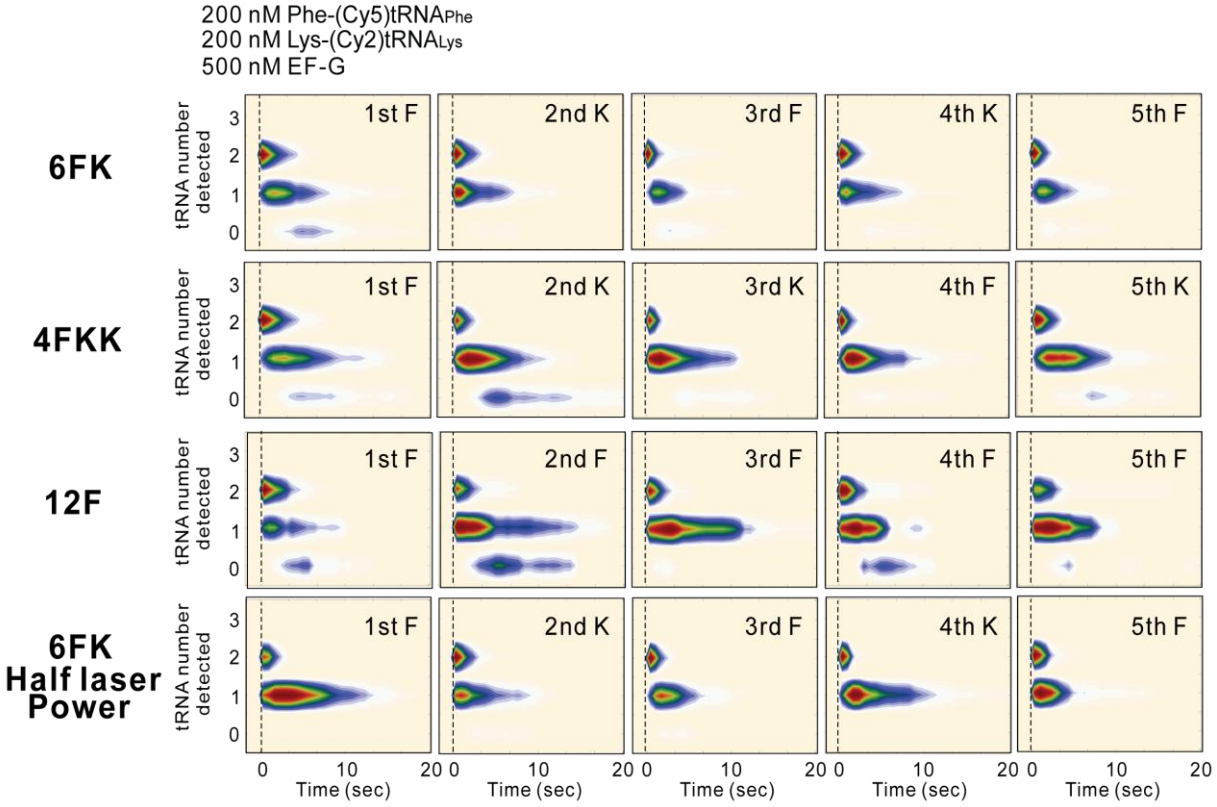

Supplementary figure. 6

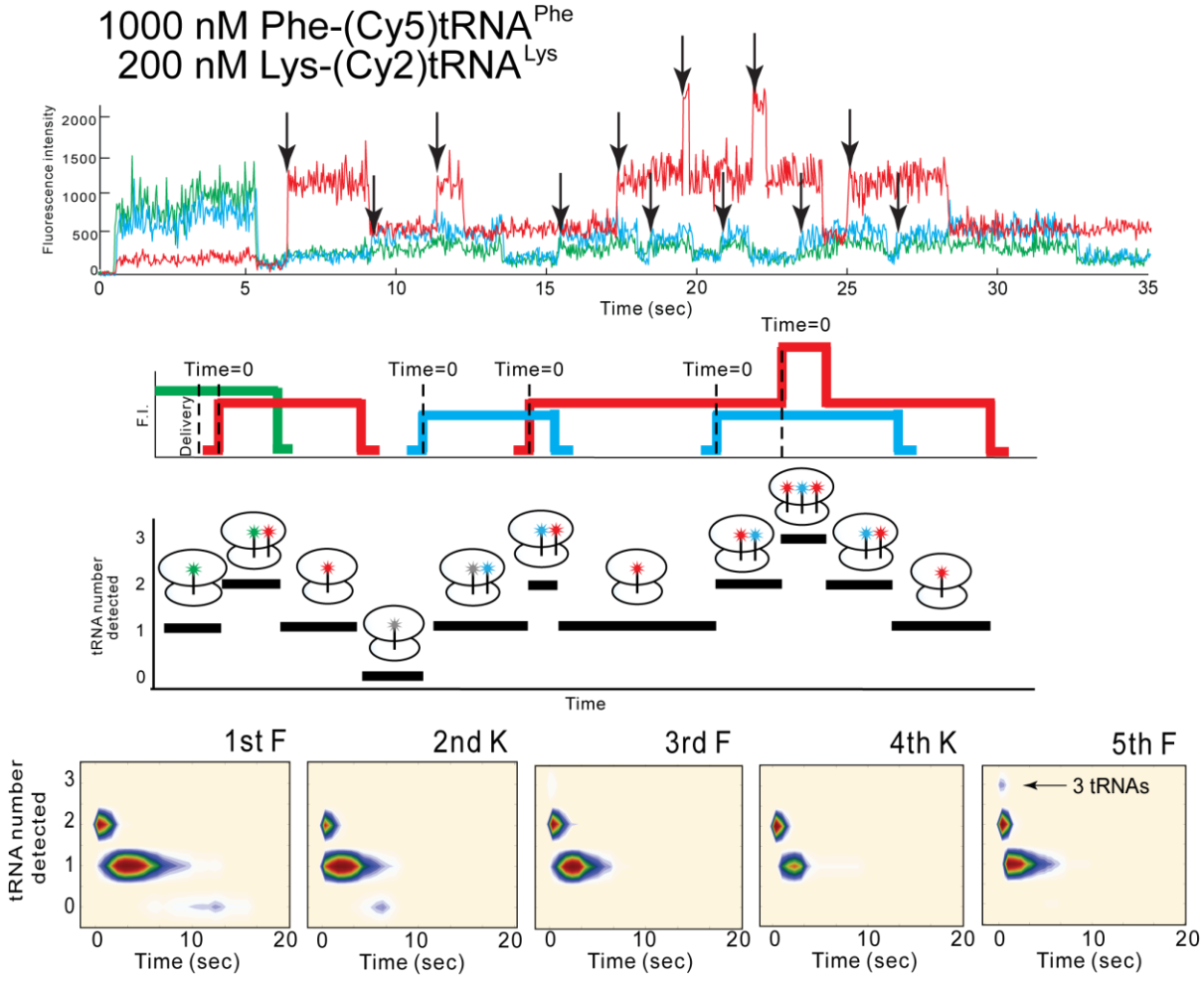

Supplementary figure. 7